

Microstructure and corrosion resistance of $\text{Al}_2\text{CrFeCoCuNi}_x\text{Ti}$ high entropy alloy coatings prepared by laser cladding

Qiu Xingwu^{1, 2, 3}, Wu Mingjun¹, Qi Yan³, Liu Chungu⁴, Zhang Yunpeng⁵, Huang Chongxiang^{2*}

(1. Innovation and Practice Base for Postdoctors, Sichuan College of Architectural Technology, Deyang 618000, China;

2. School of Aeronautics & Astronautics, Sichuan University, Chengdu 610065, China;

3. Department of Materials Engineering, Sichuan College of Architectural Technology, Deyang 618000, China;

4. Department of Surveying and Mapping Engineering, Sichuan College of Architectural Technology, Deyang 618000, China;

5. School of Material Science and Engineering, Xi'an University of Technology, Xi'an 710048, China)

Abstract: The $\text{Al}_2\text{CrFeCoCuNi}_x\text{Ti}$ high entropy alloy coating was prepared by laser cladding on Q235 steel surface. The microstructure of $\text{Al}_2\text{CrFeCoCuNi}_x\text{Ti}$ high entropy alloy coatings were analyzed, and the corrosion resistance of $\text{Al}_2\text{CrFeCoCuNi}_x\text{Ti}$ high entropy alloy coatings in 0.5 mol/L HNO_3 solution and 0.5 mol/L HCl solution were tested. The experimental results show that the $\text{Al}_2\text{CrFeCoCuNi}_x\text{Ti}$ high entropy alloy coating can be divided into cladding zone, bonding zone and heat affected zone. The microstructure of cladding zone is mainly composed of equiaxed grain, with micron-grade particles distributed on it, the phase structure of $\text{Ni}_{1.0}$ high entropy alloy coating was simple for FCC and BCC structure. Due to the passivation effect of Cr and Ni elements and formation of Al_2O_3 and $\text{Al}_2\text{O}_3 \cdot \text{H}_2\text{O}$ films by Al element, the $\text{Al}_2\text{CrFeCoCuNi}_x\text{Ti}$ high entropy alloy coating exhibits good corrosion resistance in 0.5 mol/L HNO_3 solution and 0.5 mol/L HCl solution. Compared with Q235 steel, the corrosion current density decreases 1–2 orders of magnitude. Pitting corrosion appears because of Cl^- in 0.5 mol/L HCl solution can penetrate the passive film on the $\text{Ni}_{0.5}$ high entropy alloy coating surface.

Key words: $\text{Al}_2\text{CrFeCoCuNi}_x\text{Ti}$; high entropy alloys; laser cladding; microstructure; corrosion resistance

CLC number: TN249 **Document code:** A **DOI:** 10.3788/IRLA201847.0706008

激光熔覆 $\text{Al}_2\text{CrFeCoCuNi}_x\text{Ti}$ 高熵合金涂层的组织及耐蚀性能

邱星武^{1,2,3}, 吴明军¹, 戚燕³, 刘春阁⁴, 张云鹏⁵, 黄崇湘^{2*}

(1. 四川建筑职业技术学院 博士后创新实践基地, 四川 德阳 618000; 2. 四川大学 空天科学与工程学院, 四川 成都 610065; 3. 四川建筑职业技术学院 材料工程系, 四川 德阳 618000; 4. 四川建筑职业技术学院 测绘工程系, 四川 德阳 618000; 5. 西安理工大学 材料科学与工程学院, 陕西 西安 710048)

摘要: 采用激光熔覆工艺在 Q235 钢表面制备了 $\text{Al}_2\text{CrFeCoCuNi}_x\text{Ti}$ 高熵合金涂层, 分析了 $\text{Al}_2\text{CrFeCoCuNi}_x\text{Ti}$ 高熵合金涂层的组织结构, 测试了 $\text{Al}_2\text{CrFeCoCuNi}_x\text{Ti}$ 高熵合金涂层在 0.5 mol/L

收稿日期: 2018-02-05; 修订日期: 2018-03-03

基金项目: 国家自然科学基金(11672195); 四川建筑职业技术学院科学技术研究项目(2017KJ02)

作者简介: 邱星武(1982-), 男, 副教授, 博士, 主要从事激光材料表面改性方面的研究。Email: fallenrain922@163.com

通讯作者: 黄崇湘(1977-), 男, 教授, 博士, 主要从事航空航天材料的力学行为方面的研究。Email: chxhuang@scu.edu.cn

HNO₃ 溶液及 0.5 mol/L HCl 溶液中的耐蚀性能。结果表明:Al₂CrFeCoCuNi_xTi 高熵合金涂层主要分为熔覆区、结合区、热影响区,熔覆区组织主要由等轴晶组成,等轴晶上分布有微米尺度的粒子;合金相结构简单,由体心立方(BCC)及面心立方(FCC)结构组成;Cr 元素和 Ni 元素的钝化作用及由 Al 元素形成 Al₂O₃ 或 Al₂O₃·H₂O 膜使得 Al₂CrFeCoCuNi_xTi 高熵合金涂层在 0.5 mol/L HNO₃ 溶液及 0.5 mol/L HCl 溶液中具有较好的耐蚀性能,自腐蚀电流密度与基体 Q235 钢相比降低一两个数量级;0.5 mol/L HCl 溶液中的 Cl⁻ 会穿透 Ni_{0.5} 高熵合金涂层表面形成的钝化膜,出现轻微小孔腐蚀。

关键词: Al₂CrFeCoCuNi_xTi; 高熵合金; 激光熔覆; 显微组织; 耐蚀性能

0 Introduction

The traditional alloys are in one or two kinds (such as Al, Fe, Mg, Ni, Co, Cu, etc.) metal as the mainly elements, the structure and properties depends on the mainly elements. Recently, with the rapid development of science and technology, the demand is also being more and more strict; the existing alloy has been unable to meet the actual needs. "High entropy alloy" is a new type of alloy material developed in this background. The difference with the traditional alloys lies in: high entropy alloy refers to the alloy containing a variety of major elements, which has high mole fractions of each main element, but not more than 35%, the alloy is characterized by a variety of elements collectively^[1-2]. As results, a series of excellent properties can be achieved in this kind of alloys, for instance high strength and high hardness, high wear resistance, high corrosion resistance, high temperature resistance and high resistivity etc^[3-4]. High entropy alloy can be used in many fields, such as tools, cutting tools, moulds, golf head hitting surface, motor core, hydraulic pressure rod, high frequency transformer, magnetic head, magnetic disk, turbine blades, welding materials, heat exchangers and heat resistant materials. More and more scholars have studied the structure and properties of high entropy alloys; the research involves elements selection, composition design, preparation method, microstructure transformation, strengthening mechanism^[5-6]. Although the research has made some progress, but there are still a lot of work to do.

At present, the main method for preparing high entropy alloys is vacuum arc furnace casting^[7-8], the products under the casting condition have natural defects (such as voids, osteoporosis caused by thermal expansion and contraction) the process is relatively complex, and the microstructure and properties of the high entropy alloy are difficult to control. Laser cladding method is a new method to prepare high entropy alloys. The advantage of this method is that: (1) the laser beam has high energy density, fast heating rate, and fast cooling rate. Rapid solidification refers to the rapid cooling of molten or heterogeneous nucleation, the alloy in the solidification of high growth rate of the great undercooling, therefore, can be used for the preparation of amorphous, quasicrystalline, microcrystalline and nanocrystalline alloy; (2) the coating can be obtained by laser cladding technology on the surface of traditional materials, which can improve the surface properties of the substrate material and protect the inner metal; (3) the metallurgical bonding between the coating and the substrate material.

The corrosion resistance of the material is one of the important properties that affect the service life of the material. How to protect the material surface effectively has become one of the important research directions of the experts and scholars. The preparation of laser cladding coating on the surface of the substrate provides an effective way to improve the corrosion resistance. The Al₂CrFeCoCuNi_xTi high entropy alloy coating on Q235 steel surface was prepared by laser cladding, the microstructure and corrosion resistance of the coating are mainly studied,

so as to provide references for the further study of the alloy and expand the scope of use of Q235 steel.

1 Experimental

Many scholars choose Al, Cr, Fe, Ni and Co elements as the main elements, on this basis, in order

to study the state of Cu element in high entropy alloy prepared by different processes and the effect of Ti element on high entropy alloy, Cu and Ti elements were added. Q235 steel was used as the substrate material. were used as cladding power. Table 1 shows the composition of used power.

Tab.1 Composition of Al₂CrFeCoCuNi_xTi (molar ratio)

No.	Composition	Al	Co	Cr	Cu	Fe	Ni	Ti
Ni _{0.0}	Al ₂ CoCrCuFeTi	28.6	14.3	14.3	14.3	14.3	-	14.3
Ni _{0.5}	Al ₂ CoCrCuFeNi _{0.5} Ti	26.6	13.3	13.3	13.3	13.3	6.7	13.3
Ni _{1.0}	Al ₂ CoCrCuFeNi _{1.0} Ti	25.0	12.5	12.5	12.5	12.5	12.5	12.5
Ni _{1.5}	Al ₂ CoCrCuFeNi _{1.5} Ti	23.5	11.8	11.8	11.8	11.8	17.6	11.8
Ni _{2.0}	Al ₂ CoCrCuFeNi _{2.0} Ti	22.2	11.1	11.1	11.1	11.1	22.2	11.1

The Q235 steel surface was treated by grinding machine, and then uses the cleaning acetone to remove the dirt and oil. Mixing the alloy powder in a ball mill for 24 hours and a ball-to-powder weight ratio of 10:1, and then mix thoroughly with an organic solvent, pre-coated uniformly on Q235 steel surface, the layer thickness is 1.0 mm. Laser cladding was carried out by the laser processing machine (DL-HL-T5000B). The processing parameters were: power $P=2\ 500\ W$, spot diameter $D=4\ mm$, scanning speed $V=3\ mm/s$. The corrosion resistance sample was scanned by multi pass lap, and the lap rate was 35%. Argon was used as protection gas during processing. With the different Ni content (x in Al₂CrFeCoCuNi_xTi is a molar content, the values are 0.0, 0.5, 1.0, 1.5, 2.0 respectively, following represent five alloys with Ni_{0.0}, Ni_{0.5}, Ni_{1.0}, Ni_{1.5}, Ni_{2.0} in the alloys.

Al₂CrFeCoCuNi_xTi high-entropy alloys morphology and microstructures were investigated by metallographic microscope (OM, GX71) and field emission scanning electron microscope (SEM, JSM-6700F). Chemical compositions of different micro-area were analyzed by SEM energy dispersive spectrometry(EDS). The phase composition of high entropy alloy coating was identified using an X-ray diffractometer (XRD-7000)

with Cu target, voltage 40 kV, current 40 mA, the scan range from 30° to 90°, and the scanning speed is 4 (°)/min. The potentiodynamic polarization curves and cyclic polarization curve of the studied alloys coatings and substrate in 0.5 mol/L HNO₃ solution and 0.5 mol/L HCl solution were investigated by an electrochemical workstation (CHI660 D) at room temperature, using three-electrode system, in which the saturated calomel electrode is a reference electrode, auxiliary electrode is a platinum electrode and laser alloying specimens is a working electrode (bare area: 1 cm²), the potential scan range of polarization curves in 0.5 mol/L HNO₃ solution and 0.5 mol/L HCl solution were -0.8-0.8 V and -0.8-0.6 V, respectively, the potential scan range of cyclic polarization curve in 0.5 mol/L HCl solution was -0.5-0.0 V, all the scanning rate were 1 mV/s.

2 Results and discussion

2.1 Microstructure and XRD analysis

Figure 1 shows the microstructure of Al₂CrFeCoCuNi_xTi high entropy alloy coating, in which Fig.1(a) for the morphology metallographic photo of Ni_{0.5} alloy coating. Obviously, the cladding layer has no defects, and the cross section is divided into

the cladding zone(CZ), the binding zone(BZ) and the heat affected zone (HAZ), and the following parts is the matrix.

Figure 1 (b) shows the cladding zone of Ni_{0.0} alloy. The microstructure of Al₂CrFeCoCuNi_xTi high entropy alloy coating is mainly composed of equal axial grains, and the grains are arranged closely, showing the shape of the field after drying up. The equal axial grain is the result of the free growth of the crystal nucleus in the melt. Alloy powder rapid melting into liquid under the conditions of laser rapid heating (10⁴–10⁶ °C/s), the liquid metal flow accelerates the heat dissipation of macro overheating; the micro turbulence brought strong temperature fluctuations, resulting in free grain drift and accumulation, promote the grain free, accelerated melt homogenization. As the solidification layer is in the inward passage, the heat dissipation ability of the substrate is gradually weakened, the internal temperature gradient tends to be gentle, and the solute atoms in the liquid phase are more and more enriched. The constitutional undercooling of the front surface of the interface is gradually increasing. When the constitutional undercooling is large enough to occur heterogeneous nucleation, it leads to the formation of internal and other axial grains, and provides a guarantee for the coating to obtain good performance.

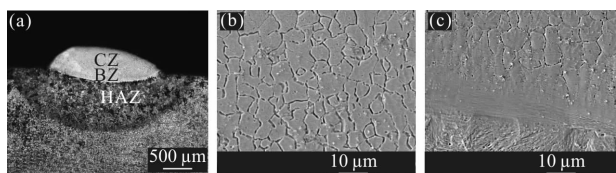


Fig.1 Microstructure morphologies of the high entropy alloy.

(a) Macroscopic feature of Ni_{0.5} alloy, (b) cladding zone of Ni_{0.0} alloy, (c) bounding zone of Ni_{2.0} alloy

Figure 1 (c) illustrate the bounding zone of Ni_{2.0} alloy. The bonding zone is the interface between the cladding coating and the substrate. The coating and the substrate are well combined. From Fig.1 (b) and Fig.1 (c) we can see that the distribution of the white precipitates on the equal axial grain, the size of

precipitates is with micron-grade. Al₂CrFeCoCuNi_xTi alloy cladding powder is melted quickly by the high energy laser beam, a variety of elements contained in the melt in disarray, the diffusion and rearrangement of the elements became much more difficult than that of the conventional alloys by the cooling effect of Q235 steel, thus forming nano scale precipitates.

Under the bonding zone is the heat affected zone, compared with the matrix, the microstructure changes due to the input of laser energy, the microstructure has become small. Under the heat affected zone is the matrix, which is still the original structure.

In order to identify the phase composition of the coating, XRD analysis of Ni_{1.0} alloy coating was carried out, the results shows in Fig.2. Due to the high entropy effect, Ni_{1.0} alloy coating formed simple face-centered cubic (FCC) and body-centered cubic(BCC) phase and does not tend to form brittle intermetallic compounds.

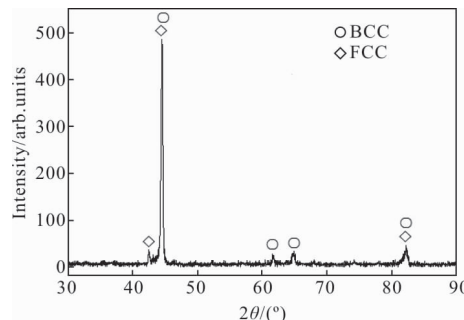


Fig.2 XRD diffraction pattern of Ni_{1.0} high entropy alloy coating

The Ni_{0.0} alloy appeared columnar crystal (Fig.3) near the bounding zone. The orientation of columnar crystals is approximately perpendicular to the surface of the substrate. Line scanning was carried out, the element distribution as shown in Fig.3. It can be concluded that the Al, Ti and Co rich in right side of the columnar crystal, while the other elements are relatively uniform. Elements segregation appeared, but the degree is slight. From the line scanning and area scanning analysis, it can be found that the Cu element does not enrich in intergranular, which is different from the previous reports^[9-10].

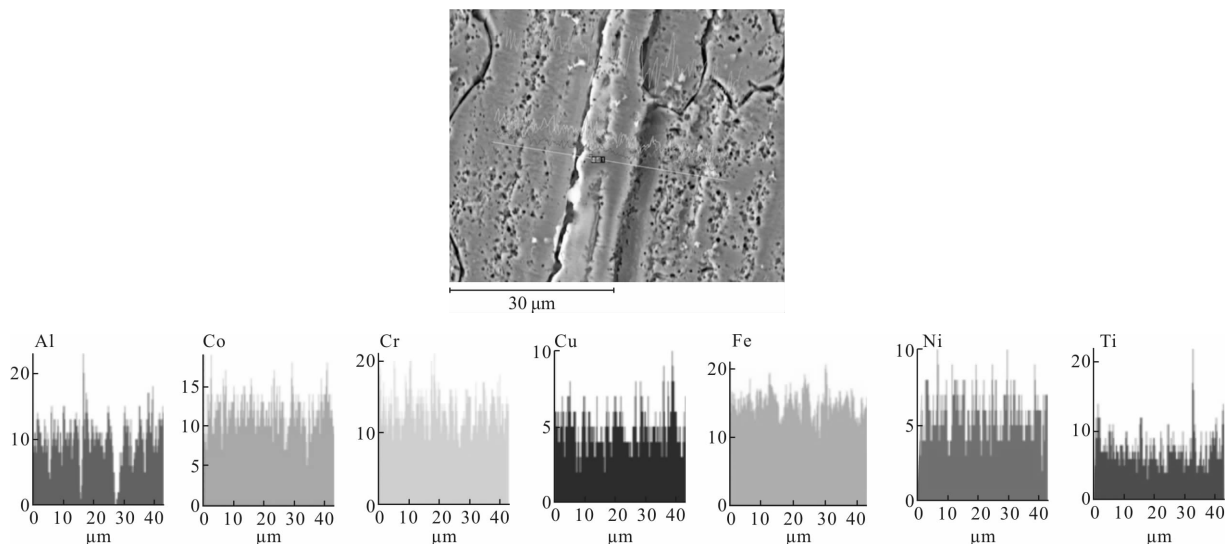


Fig.3 Elements line scanning of Ni_{0.5} high entropy alloy coating close to bounding zone

2.2 Corrosion resistance

Figure 4 illustrates the dynamic potential polarization curves of Al₂CrFeCoCuNi_xTi high-entropy alloy coating and Q235 steel in 0.5 mol/L HNO₃ solutions. The corrosion kinetic parameters obtained by the linear fitting (least squares method) are shown in Tab.2.

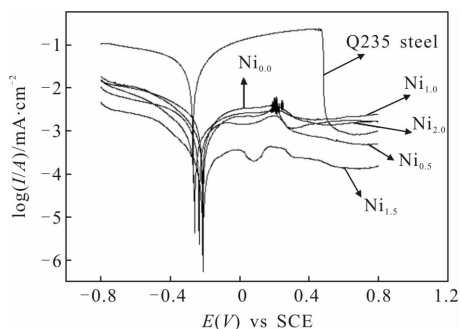


Fig.4 Polarization curves of Al₂CrFeCoCuNi_xTi high entropy alloy coatings and Q235 steel in 0.5 mol/L HNO₃ solution

Tab.2 Corrosion dynamics parameters of Al₂CrFeCoCuNi_xTi high entropy alloy coatings and Q235 steel in 0.5 mol/L HNO₃ solution

Sample	I_{corr} /mA · cm ⁻²	E_{corr}/V	I_{pp} /mA · cm ⁻²	E_{pp}/V	$R_p/k \cdot cm^2$
Q235 steel	2.4×10^{-1}	-0.35	8.1×10^{-1}	-0.11	0.56
Ni _{0.0}	2.9×10^{-2}	-0.28	4.3×10^{-2}	-0.19	1.03
Ni _{0.5}	8.2×10^{-3}	-0.29	2.2×10^{-2}	-0.12	3.72
Ni _{1.0}	7.3×10^{-3}	-0.33	1.3×10^{-2}	-0.16	4.77
Ni _{1.5}	1.4×10^{-3}	-0.26	6.6×10^{-3}	0.03	5.68
Ni _{2.0}	2.7×10^{-2}	-0.27	9.0×10^{-2}	-0.20	0.92

Visible from Fig.4, there is a clear passivation on the polarization curve. High entropy alloy coating after immersion liquid, at the beginning, with the increase of potential, current density decreases, that is the polarization curve of the left half part; when the potential is increased to a certain value, the current density decreases sharply and then increases sharply. As the potential continues to increase, the current density remains unchanged, namely into the passive region. Metals and alloys appear passivation area, indicating that the material is protected^[11-12].

According to Faraday's law:

$$Q = MF/N \tag{1}$$

In formula (1), Q expressed the power through primary battery; M is the amount of substance that changes during the t time; F is the Faraday constant, its value is 96 500 C/mol; N represents the chemical equivalent. Because:

$$Q = I_{corr}t \tag{2}$$

In formula (2), I_{corr} is the corrosion current density, from formula (1) and (2) we can get:

$$M = I_{corr}tN/F \tag{3}$$

Or as:

$$M = KI_{corr}t \tag{4}$$

In which:

$$K = N/F \tag{5}$$

The corrosion rate is the amount of substance

that changes in unit area per unit time under electrochemical action:

$$\mu = M/St = KI_{\text{corr}}/S \quad (6)$$

In formula (6) μ is the corrosion rate, S is the corrosion area.

It is indicated that the corrosion rate is proportional to the corrosion current density (I_{corr}).

From the data in Tab.2, the corrosion potential (E_{corr}) of $\text{Al}_2\text{CrFeCoCuNi}_x\text{Ti}$ high entropy alloy coating in 0.5 mol/L HNO_3 solution compared with Q235 steel "positive shift" not obvious, but the corrosion current density of high entropy alloy coating (I_{corr}) compared with Q235 steel decreased 1–2 orders of magnitude, indicating that $\text{Al}_2\text{CrFeCoCuNi}_x\text{Ti}$ high entropy alloy coating has a good corrosion resistance in 0.5 mol/L HNO_3 solution. Under the condition of rapid cooling of the laser, the grains have less time to grow up; fine and uniform equal axial grains formed, and the close arrangement of the equal axial grains provide a guarantee for obtaining good corrosion resistance. In strong oxidizing HNO_3 solution, Cr element and Ni element binding, is more conducive to passivation, and thus stable in 0.5 HNO_3 mol/L solutions. At the same time, the Al element in the $\text{Al}_2\text{CrFeCoCuNi}_x\text{Ti}$ high entropy alloy coating is easy to be passive, which can form Al_2O_3 or $\text{Al}_2\text{O}_3 \cdot \text{H}_2\text{O}$ mol/L film in 0.5 HNO_3 solution, which can effectively delay the corrosion rate. Combined with Fig.1, Tab.2 and electrochemical theory, the corrosion resistance of high entropy alloy coating in 0.5 HNO_3 solutions is in the order of $\text{Ni}_{1.5}$, $\text{Ni}_{1.0}$, $\text{Ni}_{0.5}$, $\text{Ni}_{2.0}$, and $\text{Ni}_{0.0}$.

Figure 5 shows the dynamic potential polarization

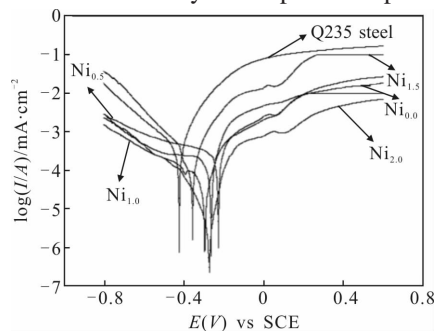


Fig.5 Polarization curves of $\text{Al}_2\text{CrFeCoCuNi}_x\text{Ti}$ high entropy alloy coatings and Q235 steel in 0.5 mol/L HCl solution

curves of $\text{Al}_2\text{CrFeCoCuNi}_x\text{Ti}$ high entropy alloy coating and Q235 steel in 0.5 HCl mol/L solutions. The corrosion kinetic parameters obtained by the linear fitting are shown in Tab.3.

Tab.3 Corrosion dynamics parameters of $\text{Al}_2\text{CrFeCoCuNi}_x\text{Ti}$ high entropy alloy coatings and Q235 steel in 0.5 mol/L HCl solution

Sample	I_{corr} /mA·cm ⁻²	E_{corr} /V	I_{pp} /mA·cm ⁻²	E_{pp} /V	R_p /k·cm ²
Q235 steel	2.1×10^{-3}	-0.41	7.1×10^{-2}	-0.26	20.25
$\text{Ni}_{0.0}$	5.8×10^{-4}	-0.24	2.3×10^{-3}	-0.09	44.60
$\text{Ni}_{0.5}$	1.2×10^{-3}	-0.22	9.2×10^{-3}	0.03	26.65
$\text{Ni}_{1.0}$	3.3×10^{-4}	-0.30	6.2×10^{-3}	-0.16	56.88
$\text{Ni}_{1.5}$	6.0×10^{-4}	-0.36	7.6×10^{-3}	-0.21	50.36
$\text{Ni}_{2.0}$	4.7×10^{-5}	-0.25	8.3×10^{-4}	-0.05	521.66

Combined with Fig.5 and Tab.3, the $\text{Al}_2\text{CrFeCoCuNi}_x\text{Ti}$ high entropy alloy coating exhibits excellent corrosion resistance in the 0.5 HCl mol/L solutions. Its corrosion current density (I_{corr}) is significantly lower than that of Q235 steel, and the maximum reduction is 2 orders of magnitude. The corrosion potential (E_{corr}) compared with that of Q235 steel is "positive shifted" by 0.05–0.19 V. This shows that the $\text{Al}_2\text{CrFeCoCuNi}_x\text{Ti}$ high entropy alloy coating has good corrosion resistance in the 0.5 HCl mol/L solutions. Ni in $\text{Al}_2\text{CrFeCoCuNi}_x\text{Ti}$ high entropy alloy coating is stable enough in dilute HCl acid at room temperature, so the coating has better corrosion resistance. But the alloy coatings with different structures, lattice distortion due to different lattice matching at the grain boundary, so that the activation energy increased, the grain boundary becomes the weakest part, acidic medium containing chloride ions, the corrosion of the grain boundary is particularly evident^[13–14].

Circular polarization curve is carried out by cyclic scanning in the fixed potential range. According to the characteristics of the curve, we can judge whether the material surface is pitting or not. The

envelope area between the positive and reverse polarization curve is called as the hysteresis area, and the envelope curve is called as the hysteresis ring. Generally, when the circular polarization curves show positive hysteresis ring, the surface of the material is pitting. The larger the area of the positive hysteresis ring, the more serious the pitting^[15]. Conversely, if the negative hysteresis ring appears in the circular polarization curve or there is no hysteresis ring, the surface of the material does not appear pitting. The area of the negative hysteresis ring is larger, suggesting that the corrosion resistance is better.

Figure 6 shows the Circular polarization curve of Ni_{0.5} high entropy alloy coating in 0.5 mol/L HCl solution. There is a positive hysteresis loop, but the area of the hysteresis loop is very small, which indicates that the Ni_{0.5} high entropy alloy coating has pitting corrosion in the 0.5 HCl mol/L solution, but the degree is slight.

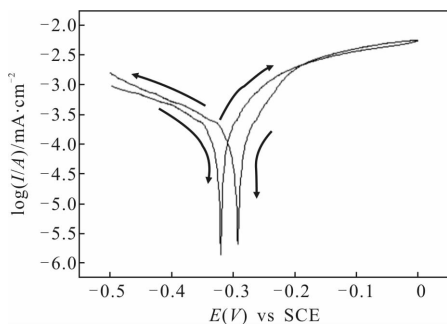


Fig.6 Circular polarization curve for Ni_{0.5} high entropy alloy coating in 0.5 mol/L HCl solution

Combined with the corrosion kinetic parameters in Tab.3, the corrosion potential of Ni_{0.5} high entropy alloy coating was 0.19 V higher than that of Q235 steel, and the corrosion current density was lower than that of Q235 steel. When $x=0.5$, the Ni content is relatively small, although the passivation film is formed on the surface, the thickness of the film is not thick enough, and the density is not large enough, the passivation film can play a protective effect on the Q235 steel surface in the HCl solution. With the extension of time, the Cl⁻ in HCl solution was first

adsorbed on some parts of the alloy coating, the penetrating effect of passive film on the coating surface is produced. The passivation film damaged parts becomes a galvanic anode, while the rest is not destroyed as part of the cathode, thus forming passivation activation cell^[16-17]. As the anode area is much smaller than the cathode area, the anode current density is very large; it will soon be etched into a small hole. At the same time, when the corrosion current flows to the cathode part of the small hole around, the part is protected by the cathode, which is maintained in a passive state. With the flow of the current, the Cl⁻ ions in solution migration into the inside of the hole, a concentrated solution of a metal chloride (e.g., FeCl₃, NiCl₃, CrCl₃, AlCl₃) is formed in a small hole, the hole surface keeps the activation status. Due to the constant hydrolysis of the chloride solution, the acidity of the solution in the small hole is increased, and the corrosion of the small hole is further intensified.

3 Conclusion

Al₂CrFeCoCuNi_xTi high entropy alloy coating is mainly divided into the cladding zone, bonded zone and heat affected zone, the microstructure of cladding zone is mainly composed of equiaxed grains, the grains are fine and uniform, closely spaced, the phase structure of Ni_{1.0} high entropy alloy coating was simple for FCC and BCC structure. The corrosion resistance of high entropy alloy coating in 0.5 HNO₃ mol/L and in 0.5 mol/L HCl solutions are excellent, and the corrosion current density is reduced by 1-2 orders of magnitude compared with that of the Q235 steel. The Ni element in Al₂CrFeCoCuNi_xTi high entropy alloy coating stable enough in dilute HCl at room temperature. The cyclic polarization curves show that the Cl⁻ in the 0.5 HCl mol/L solutions can penetrate the passive film which formed on the surface of the Ni_{0.5} high entropy alloy coating, and the pitting corrosion occurs.

References:

- [1] Yeh J W, Chang S Y, Hong Y D, et al. Anomalous decrease in X-ray diffraction intensities of Cu-Ni-Al-Co-Cr-Fe-Si alloy systems with multi-principal elements [J]. *Materials Chemistry and Physics*, 2007, 103: 41-46.
- [2] Liu Shuqian, Huang Weigang. Microstructure and mechanical performance of AlCrCoNiSix high-entropy alloys [J]. *Journal of Materials Engineering*, 2012, 40(1): 5-8. (in Chinese)
- [3] Zhang Airong, Liang Hongyu, Li Ye. Property of AlCrCoFeNiMoTi_{0.75}Si_{0.25} high-entropy alloy coating tool prepared by laser cladding [J]. *China Surface Engineering*, 2013, 26(4): 27-31. (in Chinese)
- [4] An Xulong, Liu Qibin, Zheng Bo. Microstructure and properties of laser cladding high entropy alloy MoFeCrTiWAl₂Si_y coating [J]. *Infrared and Laser Engineering*, 2014, 43(4): 1140-1144. (in Chinese)
- [5] Hu Z H, Zhan Y Z, Zhang G H. Effect of rare earth Y addition on the microstructure and mechanical properties of high entropy AlCoCrCuNiTi alloys[J]. *Materials and Design*, 2010, 31: 1599-1602.
- [6] Tang Qunhua, Liao Xiaozhou, Dai Pinqiang. Microstructure evolution of Al_{0.3}CoCrFeNi high-entropy alloy during high-pressure torsion [J]. *Journal of Materials Engineering*, 2015, 43(12): 45-51. (in Chinese)
- [7] Hsu C Y, Sheu T S, Yeh J W, et al. Effect of iron content on wear behavior of AlCoCrFexMo_{0.3}Ni high-entropy alloys [J]. *Wear*, 2009, 268: 653-659.
- [8] Shun T T, Hung C H, Lee C F. The effects of secondary elemental Mo or Ti addition in Al_{0.3}CoCrFeNi high-entropy alloy on age hardening at 700 °C [J]. *Journal of Alloys and Compounds*, 2010, 495: 55-58.
- [9] Hsu Y J, Chiang W C. Corrosion behavior of FeCoNiCrCux high-entropy alloys in 3.5% sodium chloride solution [J]. *Materials Chemistry and Physics*, 2005, 92: 112-117.
- [10] Xie Hongbo, Liu Guizhong, Guo Jingjie. Effect of Zr addition on microstructure and corrosion properties of AlFeCrCoCuZrx high-entropy alloys[J]. *Journal of Materials Engineering*, 2016, 44(6): 44-49. (in Chinese)
- [11] Ma Chen, Ma Zhuang, Gao Lihong, et al. Laser damage mechanism of flake graphite modified phenolic resin coating [J]. *Chinese Optics*, 2017, 10(2): 249-255. (in Chinese)
- [12] Pham Thihongnga, Liu Hongxi, Zhang Xiaowei, et al. Microstructure and high-temperature wear behaviors of Co/TiC laser coatings on die steel [J]. *Optics and Precision Engineering*, 2013, 21(8): 2048-2055. (in Chinese)
- [13] Liu Hongxi, Tao Xiaode, Zhang Xiaowei, et al. Microstructure and interface distribution of Fe-Cr-Si-B-C laser cladding alloy coatings assisted by mechanical vibration[J]. *Optics and Precision Engineering*, 2015, 23(8): 2192-2202. (in Chinese)
- [14] Chou Y L, Wang Y C, Yeh J W. Pitting corrosion of the high-entropy alloy Co_{1.5}CrFeNi_{1.5}Ti_{0.5}Mo_{0.1} in chloride-containing sulphate solutions [J]. *Corrosion Science*, 2010, 52: 3481-3491.
- [15] Wang Xuede, Luo Sihai, He Weifeng, et al. Effects of laser shock processing without coating on mechanical properties of K24 nickel based alloy [J]. *Infrared and Laser Engineering*, 2017, 46(1): 0106005. (in Chinese)
- [16] Zhang Min, Liu Chang, Ren Bo, et al. Microstructure and mechanical properties of porous Ni alloy fabricated by laser 3D printing [J]. *Chinese Optics*, 2016, 9(3): 335-341. (in Chinese)
- [17] Liu Hongxi, Leng Ning, Zhang Xiaowei, et al. Microstructure and wear behavior of WC/Co50 composite coatings on 40Cr cutting tool surface prepared by laser cladding [J]. *Infrared and Laser Engineering*, 2016, 45(1): 0106005. (in Chinese)